

## Examination of antibacterial properties of pure and aluminum doped zinc oxide nanoparticles

N. Srinivasan<sup>1\*</sup> J. C. Kannan<sup>2</sup> and S. Satheeskumar<sup>3</sup>

<sup>1\*</sup>Department of Physics, Kongu engineering college, Perundurai, Erode, Tamilnadu, India-638 058.

<sup>2</sup>Department of Physics, KSR Institute for engineering and technology, Tiruchengode-637 215, India

<sup>3</sup>Department of Physics, Sri Shanmugha College of engineering and Technology, Sankari, Salem-637304, India

**Abstract:** The present examination aimed to prepare pure and aluminum doped zinc oxide nanoparticles by soft chemical method. The structure of the samples was confirmed through powder XRD technique as hexagonal wurtzite. Scherrer formula was used to estimate particle size of samples. The size of the particles was found in between 21 nm - 22 nm. The surface morphology was analyzed from SEM images. The spherical shaped particles were observed in SEM images. Antibacterial activities of prepared samples were probed.

**Key words:** ZnO nanoparticles, Antibacterial activity and Soft chemical method.

### 1. Introduction

Nanotechnology is an emerging area for developing new materials at nano scale. Zinc oxide nanoparticles are cost effective n-type semi conductors with hexagonal wurtzite structure [1]. Zinc oxide nanoparticles have high surface-to-volume ratio, increased reactivity and special electronic properties [2]. The properties of zinc oxide nanoparticles are enhanced by doping elements such as Al [3], Mg [4], and Ni [5]. Several methods have been used for synthesis of zinc oxide nanoparticles such as thermal evaporation [6], microwave method [7], chemical synthesis [8]. Zinc oxide nanoparticles exhibit excellent antibacterial properties [9-11]. The present study is aimed on soft chemical synthesis of pure and aluminium doped zinc oxide nanoparticles, characterization and examination of their antibacterial properties.

### 2. Experimental details

#### 2. 1. Preparation and characterization

Analytical grade reagents obtained from Merck chemicals were used without further purification. Zinc nitrate hexahydrate ( $Zn(NO_3)_2 \cdot 6H_2O$ ), aluminum nitrate nano hydrate ( $Al(NO_3)_3 \cdot 9H_2O$ ) were used as host and dopant precursors. Sodium hydroxide (NaOH) and pure de-ionized water were used in precursor solutions. Pure (S1) and aluminum doped (S2) zinc oxide nanoparticles were prepared by soft chemical method. The precursor solution was allowed for 24 hours reaction time at room temperature. The resulting precipitate was purified with de-ionized water. It was dried at air for 3 hours for the preparation of nanoparticles and growth temperature was chosen as 120 °C. Synthesized nanoparticles were characterized by XRD analysis, Scanning electron microscopy and Fourier-transform infrared spectroscopy.

## 2. 2. Antibacterial Activity

Antibacterial activities of prepared nanoparticles were tested against the bacterial strains *Staphylococcus aureus*, *Pseudomonas aeruginosa*, *Salmonella typhimurium* and *Klebsiella pneumonia* by disc diffusion method. The diameter of zone of inhibition of the sample was estimated.

## 3. Results and discussion

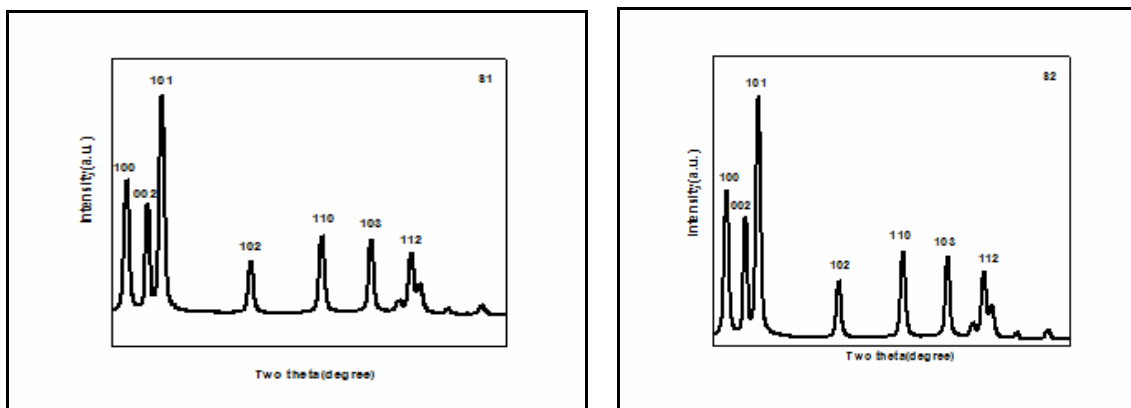
### 3. 1. XRD Analysis

Figure 1 shows the XRD patterns of pure and aluminum doped zinc oxide nanoparticles. The XRD analysis uncovered that the samples were crystallized in hexagonal wurtzite structure with space group  $P6_3mc$  (JCPDS card number 80-0075). The presence broadened diffraction peaks showed the formation of excellent nanoparticles. The absence of diffraction peak linked with aluminum pointed that the doping of aluminum has not altered the structure of zinc oxide [3]. The lattice parameters were estimated using equation (1) and (2) [1].

$$a = \frac{\lambda}{\sqrt{3}} (\sin \theta_{100}) \quad (1)$$

$$c = \frac{\lambda}{\sin \theta_{102}} \quad (2)$$

Where,  $\lambda$  and  $\theta$  were wavelength of X-ray and Bragg angle of the diffraction peak.



**Figure 1. XRD patterns of zinc oxide nanoparticles: (S1) pure, (S2) aluminum doped**

The derived values of  $a$  and  $c$  were agreed well with standard values ( $a = 3.253 \text{ \AA}$ ,  $c = 5.206 \text{ \AA}$ , JCPDS card no 80-0075). The  $c/a$  ratio values exposed that the prepared nanoparticles were high-quality crystalline structure. The calculated unit cell volumes were synchronized well with reported value ( $V=47.77 \text{ \AA}^3$  for JCPDS card number 80-0075). The lattice shrinkage was found in sample (S2) due to incorporation of aluminum in zinc oxide lattice. The diffraction peaks (100), (002) and (101) were high intensity whereas the peaks (102), (110) and (112) were less in intensity. These peaks from the patterns validated the formation of hexagonal wurtzite structure of prepared nanoparticles.

**Table 1. Parameters estimated from XRD data**

Sample	$a \text{ \AA}$	$c \text{ \AA}$	$c/a$	$V \text{ \AA}^3$	$D \text{ nm}$
S1	3.254	5.206	1.600	47.73	21
S2	3.244	5.198	1.602	47.37	22

The particle size of prepared nanoparticles was calculated by scherrer equation [10].

$$D = \frac{0.9 \lambda}{\beta \cos \theta} \quad (3)$$

Where,  $D$  and  $\beta$  were particle size and full-width at half-maximum respectively. The Gaussian fitting program was used to measure full-width at half-maximum. The particles size of prepared nanoparticles was found 21 nm (S1) and 22 nm (S2).

### 3.2. SEM Analysis

Figure 2 shows SEM micrographs of prepared nanoparticles. The SEM analysis of prepared samples probed the surface morphology. The spherical shaped nanoparticles were formed in S1. The addition of Al in sample S2 enhanced the formation of spherical nanoparticles. The aggregation of the surface was originated from the high surface energy of the nanoparticles [1].

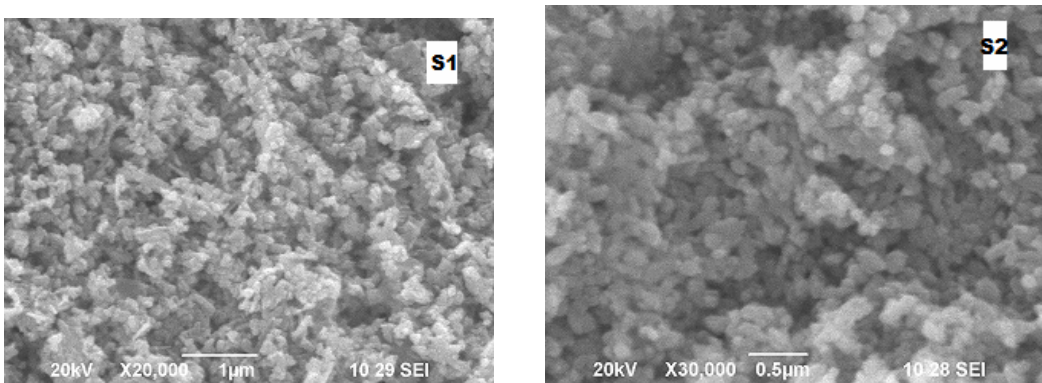


Figure 2. SEM micrographs of zinc oxide nanoparticles: (S1) pure, (S2) aluminum doped

### 3.3. FTIR Analysis

Figure-3 shows the FTIR spectra of prepared nanoparticles. Presence of different chemical functional groups established the formation of nanoparticles. The observed peaks were listed in Table 2. The stretching modes of Zinc oxide was confirmed with peaks at 454  $\text{cm}^{-1}$  and 498  $\text{cm}^{-1}$  of the samples (S1, S2)[3]. The incorporation of in Zinc oxide lattice was proved with presence of an absorption peak at 892  $\text{cm}^{-1}$  in the sample (S2). The peaks around 1400  $\text{cm}^{-1}$  and 3400  $\text{cm}^{-1}$  were assigned to OH - bending and OH – stretching modes of vibrations.

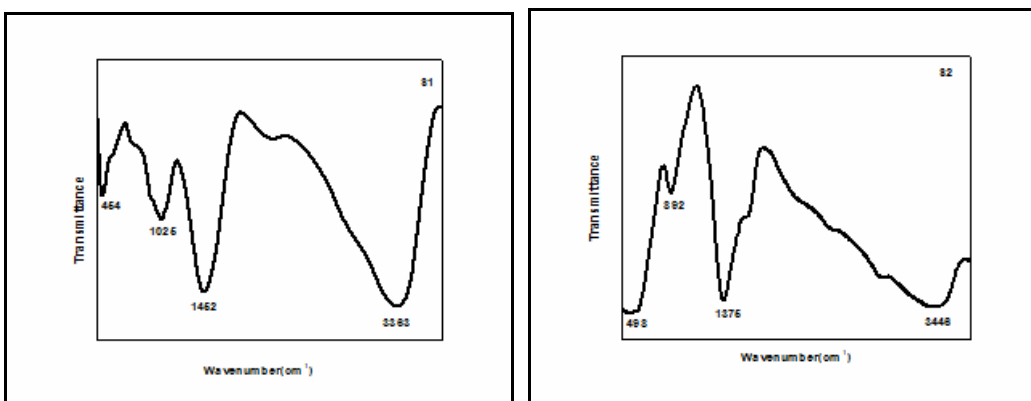


Figure 1. FTIR spectra of zinc oxide nanoparticles: (S1) pure, (S2) aluminum doped

Table 2. Chemical Functional groups assignment of FT-IR spectra

Assignment	Functional groups ( $\text{cm}^{-1}$ )	
	S1	S2
Zn-O stretching	454	498
Al-O stretching	---	892
C=O	1025	-
OH- bending	1452	1376
OH- stretching	3363	3448

### 3.4. Antibacterial Studies

The disc diffusion method was employed in antibacterial studies of prepared nanoparticles. The antibacterial activity of the nanoparticles was tested against the strains *Staphylococcus aureus*, *Pseudomonas aeruginosa*, *Salmonella typhimurium* and *Klebsiella pneumonia*. The Zone of inhibition diameter values of the nanoparticles were determined and tabulated in Table 3.

**Table 3. Zone of inhibition diameter of zinc oxide nanoparticles (mm)**

Strains	Zone of Inhibition diameter (mm)							
	S1				S2			
	25	50	75	100	25	50	75	100
<i>Staphylococcus aureus</i>	5	6	7	9	6	14	15	16
<i>Pseudomonas aeruginosa</i>	8	11	12	14	10	12	13	15
<i>Salmonella typhimurium</i>	11	14	16	17	6	12	14	15
<i>Klebsiella pneumonia</i>	7	9	12	13	7	8	10	12

The mechanism of antibacterial activity was elucidated in many research works [9-11]. The entry of nanoparticles in cell membrane was reported for the reason of massive cell death [9]. The prepared nanoparticles were highly reactive due to their high surface-to-volume ratio. The formation reactive oxygen species (ROS) was responsible for the increase in the permeability of the cell membrane. The increase in permeability of membrane brought a distribution of activity of cell membrane and enables the cell death. The DNA code of the micro-organisms was also affected by the nanoparticles [9]. The prepared nanoparticles showed better growth inhibition against the bacterial strains.

The zone of Inhibition diameter values were measured for four different concentrations (25, 50, 75 and 100  $\mu\text{g/ml}$ ). The bacterial inhibition was increased with increase in the concentration of nanoparticles. *Staphylococcus aureus* and *Pseudomonas aeruginosa* were gram-positive bacterium. *Salmonella typhimurium* and *Klebsiella pneumonia* were gram-negative bacteriums. The pure zinc oxide nanoparticles were effective on gram-negative bacteriums. The aluminium doped zinc oxide nanoparticles were highly efficient on gram-positive bacterium. The antibacterial effect of pure zinc oxide (S1) was stronger on salmonella typhimurium than other strains. The antibacterial effect of aluminium doped zinc oxide (S2) was superior on *Pseudomonas aeruginosa* than other strains.

### 4. Conclusion

Pure and aluminum doped zinc oxide nanoparticles were prepared by soft chemical method. The particles size of prepared nanoparticles was found 21 nm (S1) and 22 nm (S2) in XRD analysis. The spherical shaped particles were observed in SEM micrographs. The FTIR spectra predicted the presence of metal-oxygen bond in the samples. Antibacterial effect of nanoparticles was tested against *Staphylococcus aureus*, *Pseudomonas aeruginosa*, *Salmonella typhimurium* and *Klebsiella pneumonia*. The diameter of zone of inhibition was improved with the increase in the concentration. The increase in permeability of membrane enables the cell death. The prepared nanoparticles showed better growth inhibition against all the bacterial strains.

### References

1. Davood Raoufi, Renewable Energy. 50, 932 (2013).
2. Awodugba Ayodeji Oladiran, and Ilyas Abdul-Mojeed Olabisi, Asian Journal of Natural & Applied Sciences. 2(2), 141 (2013).
3. K. Saravanakumar, and K. Ravichandran, Journal Materials Science: Mater Electron 23, 1462 (2012).
4. C. Justin Raj, S. N. Karthick, K. V. Hemalatha, Min-Kyu Son, Hee-Je Kim, and K.Prabakar, Journal of Sol-Gel Science and Technology. 62, 453 (2012).
5. V. Pazhanivelu, A. Paul Blessington Selvadurai, and R. Murugaraj, Journal of Superconductivity and Novel Magnetism. (2014).
6. Jinfang Kong, Donghua Fan, and Yufu Zhu, Materials Science in Semiconductor Processing. 15, 258 (2012).

7. T. Krishnakumar, R. Jayaprakash, N. Pinna, N. Donato, A. Bonavita, G. Micali, and G. Neri, *Sensors and Actuators B*. 143, 198 (2009).
8. P. K. Giri, S. Bhattacharyya, B. Chetia, B. K. Panigrahi, K. G. M. Nair, and P. K. Iyer, *Journal of Nanoscience and Nanotechnology*. 8, 1 (2008).
9. Neha Sharma, Jitender Kumar, Shaveta Thakur, Shruti Sharma, and Vikas Shrivastava, *Drug Invention Today*. 5, 50 (2013).
10. Issa M. El-Nahhal, Shehata M. Zourab, Fawzi S. Kodeh, Abdelraouf A. Elmanama, Mohamed Selmane, Isabelle Genois, and Florence Babonneau. *Journal of Materials Science: Mater Electron*. 24, 3970 (2013).
11. Jasmina Vidic, Slavica Stankic, Francia Haque, Danica Ciric, Ronan Le Goffic, Aurore Vidy, Jacques Jupille, and Bernard Delmas, *Journal of Nanoparticle Research*. 15, 1595 (2013).

\*\*\*\*\*